

Cell boundary element methods for elliptic problems

Youngmok JEON and Eun-Jae PARK

(Received January 24, 2007; Revised May 2, 2007)

Abstract. In this review we summarize the results on the cell boundary element methods (CBE methods) and the multiscale cell boundary element method (MsCBE method) based on papers by Jeon and his colleagues. In the CBE methods, flux is conserved on each cell and normal fluxes on intercell boundaries are continuous for unstructured triangulations. The CBE method can be understood as an finite element version of the finite volume method.

Key words: CBE, FVM, multiscale, MsCBE, MsFEM, NcFEM.

1. Introduction

We consider the following elliptic problem:

$$\begin{aligned} -\nabla \cdot (a \nabla u) &= f & \text{in } \Omega \\ u &= 0 & \text{on } \partial\Omega, \end{aligned} \tag{1.1}$$

where a is a piecewise continuous, positive definite, symmetric tensor, $f \in H^0(\Omega)$ and Ω is a convex, bounded polygonal domain. When a is a highly oscillatory coefficients with different scales we call the problem as a multiscale problem.

In this review we introduce the cell boundary element(CBE) methods and its multiscale version(the multiscale cell boundary element(MsCBE) method) for multiscale problems, which are developed by author and his colleagues [9, 10, 11, 12, 13]. According to their researches the cell boundary element(CBE) method has the following characteristics.

- The CBE methods as well as the MsCBE method conserve flux on each cell and normal flux is continuous on each cell interface.
- They provide natural flux recovery formulas for a broad class of elliptic equations. Therefore, it may have advantage over the nonconforming finite element method(NcFEM) in terms of flux recovery formula.

2000 Mathematics Subject Classification : 65N30, 35B27, 74Q15.

The research of Y. Jeon was supported by KOSEF R01-2006-000-10472-0

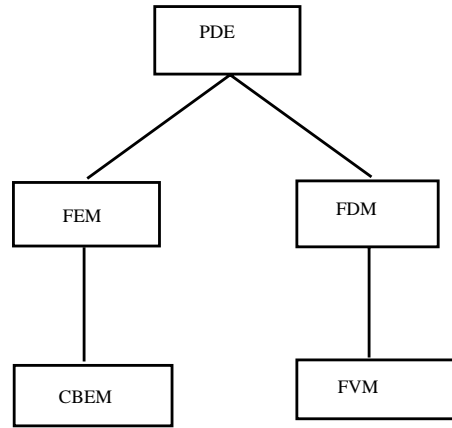


Fig. 1. Relation of the CBE methods with existing methods

- The CBE methods are very similar in view of flux oriented derivation to the finite volume method(FVM) except that they do not need covolume generations. Therefore, the CBE methods may be more flexible in mesh generation than the finite volume methods, especially in three dimensional cases. Moreover, the CBE approach introduces the 2nd order flux preserving methods naturally.

We refer to [3] and [4, 15] for more general accounts on the finite element and finite volume methods, respectively.

Figure 1 represents the relation of the CBE method with other existing methods. The CBE methods can be interpreted as an finite element version of the finite volume methods. The conforming CBE method was firstly introduced and analysed in [13, 12]. In here flux continuity on intercell boundaries is satisfied only when some special condition is satisfied by the triangulation. The CBE for the convection diffusion equation is successfully introduced in [10]. It is observed numerically that the CBE approach provides a nonoscillatory numerical scheme for convection diffusion equations. Recently, the nonconforming CBE methods are introduced and analysed in [11]. For the nonconforming CBE flux conservation for arbitrary subdomain holds for unstructured meshes. More recently, the multiscale CBE method based on the oversampling technique is introduced and analysed in [9]. The aim of this paper is to review the latest results on the CBE methods; that is, the nonconforming CBE methods and the MsCBE method.

Let \mathcal{T}_h be the triangulation of Ω and let \mathcal{E}_h be set of edges in \mathcal{T}_h . We

denote by \mathcal{N}_h and \mathcal{N}_h^i midpoints of edges and midpoints of interior edges, respectively. Then there exists a bijection between \mathcal{N}_h and \mathcal{E}_h . The skeleton of a triangulation \mathcal{T}_h is

$$\mathcal{K}_h = \bigcup_{e \in \mathcal{E}_h} e.$$

To introduce the CBE method we firstly approximate Eqn (1.1) as follows.

$$\begin{aligned} -\nabla \cdot (a_h \nabla u) &= f_h & \text{in } \Omega \\ u &= 0 & \text{on } \partial\Omega. \end{aligned} \tag{1.2}$$

Here, a_h is the piecewise constant approximation of a on each $T \in \mathcal{T}_h$ and f_h is the flux preserving approximation of f such that

$$f_h|_T = \begin{cases} \frac{1}{|T|} \int_T f dx, & \text{piecewise constant approximation,} \\ P_h(f) + \frac{1}{|T|} \int_T (f - P_h(f)) dx, & \text{piecewise linear approximation.} \end{cases}$$

Here, $P_h(f)$ can be a linear interpolation of f or a L_2 projection of f by linear functions on T .

2. The P_1 nonconforming cell boundary element method

For the nonconforming P_1 method we have a complete numerical analysis [11]. It provides a very natural flux recovery formula even when a is in a tensor form.

To derive the CBE we consider the localized problem of (1.2):

$$\begin{aligned} -\nabla \cdot (a_h \nabla u) &= f_h & \text{in } T, \\ [(a_h \nabla u) \cdot \nu] &\equiv (a_h \nabla u) \cdot \nu + (a'_h \nabla u) \cdot \nu' = 0 & \text{on } e_p = \partial T \cap \partial T', \end{aligned} \tag{2.1}$$

where ν and ν' are the unit outward normal vectors on ∂T and $\partial T'$, respectively. The solution u of (1.2) admits the following decomposition:

$$u = v + G(f_h) \quad \text{on } T. \tag{2.2}$$

Here v satisfies $-\nabla \cdot (a_h \nabla v) = 0$ on T and $v = u$ on ∂T , and $G(f_h)$ is a Green bubble function such that $-\nabla \cdot (a_h \nabla (G(f_h))) = f_h$. Then we have

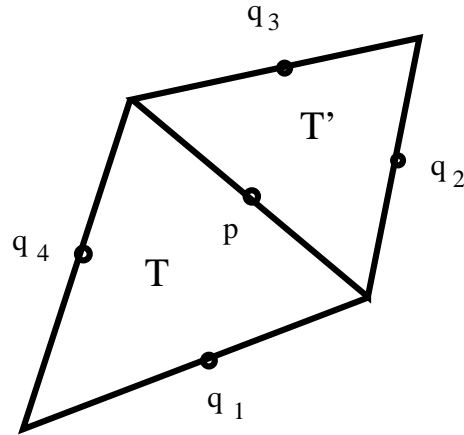


Fig. 2. A problem domain: $\Omega_h(p)$

$$[(a_h \nabla u) \cdot \nu] = [(a_h \nabla v) \cdot \nu] + [(a_h \nabla G(f_h)) \cdot \nu] \quad \text{on } \partial T.$$

Using flux continuity on cell interfaces, we have

$$\int_{e_p} [(a_h \nabla v) \cdot \nu] ds = - \int_{e_p} [(a_h \nabla G(f_h)) \cdot \nu] ds, \quad p \in \mathcal{N}_h^i, \quad (2.3)$$

where e_p is the edge related to $p \in \mathcal{N}_h^i$.

Introduce the nonconforming P_1 approximation space for v :

$$S_T = \text{span}\{1, x, y\},$$

$$S_h = \{v \in \oplus_{T \in \mathcal{T}_h} S_T : v \text{ is continuous at midpoints of edges}\}.$$

Note that $v \in S_T$ satisfies $-\nabla \cdot (a_h \nabla v) = 0$ on T and we call S_T as the space of harmonic polynomials. The natural interpolations $I_{h,T} : C(\bar{T}) \rightarrow S_T$ and $I_h : C(\bar{\Omega}) \rightarrow S_h$ are called as the *harmonic interpolation*. As long as there is no confusion, we denote $I_{h,T}$ by I_h for notational simplicity.

Now we consider approximation of the bubble function $G(f_h)$. Let $a_h = \begin{bmatrix} a_{11} & a_{12} \\ a_{21} & a_{22} \end{bmatrix}$ on certain T . Then we can take, in the two dimensional case,

$$F(f_h) = \frac{d_0}{2(a_{11} + a_{22})}(x^2 + y^2) + \frac{d_1}{6a_{11}}x^3 + \frac{d_2}{6a_{22}}y^3$$

for $f_h = d_0 + d_1x + d_2y$. Then, $(F(f_h) - I_h(F(f_h)))$ satisfies $-\nabla \cdot (a_h \nabla (F(f_h) - I_h(F(f_h)))) = f_h$ and it approximates $G(f_h)$.

The P_1 CBE method is to find $v_h \in S_h$ such that

$$\int_{e_p} [(a_h \nabla v_h) \cdot \nu] ds = - \int_{e_p} [(a_h \nabla (F(f_h) - I_h F(f_h))) \cdot \nu] ds, \quad p \in \mathcal{N}_h^i. \quad (2.4)$$

After solving v_h , we have approximate solution u_h and its flux as follows:

$$\begin{aligned} u_h &= v_h + (F(f_h) - I_h(F(f_h))), \\ a_h \nabla u_h &= a_h \nabla v_h + a_h \nabla (F(f_h) - I_h(F(f_h))). \end{aligned}$$

3. Flux conservation and numerical analysis

Note that

$$(a_h \nabla u_h) \cdot \nu = (a_h \nabla v_h) \cdot \nu + (a_h \nabla G(f_h)) \cdot \nu \quad \text{on } \partial T.$$

By definition of the P_1 CBE method,

$$\int_{e_p} (a_h \nabla u_h) \cdot \nu ds + \int_{e_p} (a'_h \nabla u_h) \cdot \nu' ds = 0.$$

Let D be arbitrary subdomain composed of triangles, simple Calculation yields

$$\begin{aligned} \int_{\partial D} (a_h \nabla u_h) \cdot \nu ds &= \sum_{T \subset D} \int_{\partial T} (a_h \nabla u_h) \cdot \nu ds \\ &= - \int_D f dx. \end{aligned}$$

Now we introduce some results on numerical analysis. Introducing a piecewise constant test function on \mathcal{K}_h , Eqn (2.4) can be rewritten as

$$\int_{\mathcal{K}_h} [(a_h \nabla v_h) \cdot \nu] \bar{\phi}_p ds = \int_{\mathcal{K}_h} [(a_h \nabla (I_h(F) - F)) \cdot \nu] \bar{\phi}_p ds, \quad p \in \mathcal{N}_h^i \quad (3.1)$$

where ϕ_p is the local basis function of S_h and $\bar{\phi}_p$ is a piecewise constant function on \mathcal{K}_h such that $\bar{\phi}_p = (1/|e|) \int_e \phi_p ds$ on each edge $e \subset \mathcal{K}_h$. The following theorem asserts that the CBE has the same stiffness matrix as the Crouzeix-Raviart P_1 finite element method and the right hand side is

different by D_h [3]. The following two theorems are from [11], where the proofs are given for the case that a is a scalar function.

Theorem 3.1 *The stiffness matrix and the right hand side of the equation (3.1) satisfy the following relations:*

$$\int_{\mathcal{K}_h} [(a_h \nabla v_h) \cdot \nu] \bar{\phi}_p ds = \sum_{T \in \mathcal{T}_h} \int_T (a_h \nabla v_h) \cdot \nabla \phi_p dx.$$

and

$$\int_{\mathcal{K}_h} [(a_h \nabla (I_h(F) - F)) \cdot \nu] \bar{\phi}_p ds = \sum_{T \in \mathcal{T}_h} \int_T f_h \phi_p dx + D_h(f_h, \phi_p),$$

where

$$D_h(f_h, \phi_p) = \sum_{T \in \mathcal{T}_h} \int_{\partial T} (a_h \nabla (I_h(F) - F)) \cdot \nu (\bar{\phi}_p - \phi_p) dx.$$

Theorem 3.2 *For $f \in L_2(\Omega)$, let u be the exact solution of (1.1) and u_h be the P_1 CBE approximate solution. Then we have an error estimate*

$$\|u_h - u\|_{1,h} \leq Ch \|f\|_{0,\Omega}.$$

Here, $\|g\|_{1,h} = \sum_{T \in \mathcal{T}_h} \|g\|_{1,T}$.

Proof. Comparison with the Crouzeix-Raviart P_1 FEM yields the theorem. \square

4. The second order methods

In this section we introduce the 2nd order method, the *harmonic* P_2^* method and its modified method, the *modified harmonic* P_2^* method. At present the second order methods are available only when the coefficient a is a piecewise constant scalar function. Convergence analysis is not available and the second order convergence is observed only experimentally.

When a is a piecewise constant scalar function ($a = a_h$), the localized problem of (1.2) becomes:

$$\begin{aligned} -a\Delta u &= f_h \quad \text{in } T, \\ \left[a \frac{\partial u}{\partial \nu} \right] &= 0 \quad \text{on } e_p = \partial T \cap \partial T'. \end{aligned} \tag{4.1}$$

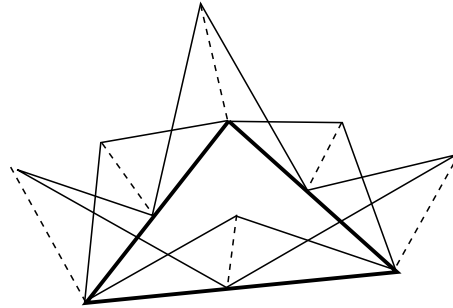


Fig. 3. Basis functions for the test function space W_h on a triangle T

Then $u = v + G(f_h)$, where v is harmonic on T with $v = u$ on ∂T and $G(f_h)$ is the Green bubble function that satisfies $-\Delta G(f_h) = f_h/a$. For approximation of v with the six-point interpolation, it is very natural to consider the space spanned by harmonic polynomials of degree of freedom six. For $G(f_h)$, f_h must be approximated by a volume preserving linear function for the second order convergence.

$$S_T = \text{span}\{1, x, y, xy, x^2 - y^2, x^3 - 3xy^2\},$$

$$S_h = \{v_h \mid v_h \in \oplus_{T \in \mathcal{T}_h} S_T, v_h \text{ is continuous at each node}\}.$$

Let I_h be the natural interpolation from $C(\bar{T})$ to S_T . To obtain the desired 2nd order convergence we need to introduce test function spaces and this fact is observed numerically. The test function space W_h is the P_1 functions on the skeleton \mathcal{K}_h (see Fig. 3). Then the harmonic P_2^* CBE method is to find $v_h \in S_h$ such that

$$\int_{\mathcal{K}_h} \left[a \frac{\partial v_h}{\partial \nu} \right] \psi_p ds = - \int_{\mathcal{K}_h} \left[a \frac{\partial (F(f_h) - I_h(F(f_h)))}{\partial \nu} \right] \psi_p ds,$$

$$\psi_p \in W_h. \quad (4.2)$$

Then $u_h = v_h + (F(f_h) - I_h(F(f_h)))$ is the solution we are looking for. In the above method flux is conserved in each cell, but average flux is not continuous at the cell interfaces. Therefore, we need to modify the test function space to have a flux conserving numerical scheme. The modified harmonic P_2^* CBE method is obtained by replacing W_h in (4.2) with W'_h , which is defined as follows:

$$W'_h = \text{span}\{\psi'_p \mid \psi'_p = \psi_p \text{ for } p, \text{ a vertex of a triangle } T \text{ and}$$

$$\psi'_p = \overline{\psi_p} \text{ for } p, \text{ a mid edge point of a triangle } T \text{ for } \psi_p \in W_h\}.$$

Then the modified harmonic P_2^* CBE method preserves flux in arbitrary subdomain.

5. A multiscale elliptic problem and the oversampling technique

We consider the following multiscale elliptic problem:

$$\begin{aligned} L_\epsilon(u_\epsilon) &= -\nabla \cdot (a_\epsilon \nabla u_\epsilon) = f && \text{on } \Omega, \\ u_\epsilon &= 0 && \text{on } \partial\Omega, \end{aligned} \quad (5.1)$$

where a_ϵ is a ϵ -periodic, positive definite, symmetric tensor. Then the solution u_ϵ has an expansion:

$$u_\epsilon(x) = u_0(x, y) + \epsilon(u_1(x, y) + \theta^{u_\epsilon}) + O(\epsilon^2) \quad (5.2)$$

where $y = x/\epsilon$. The homogenized solution u_0 and u_1 , θ^{u_ϵ} satisfy the following relations [2, 14].

$$\begin{aligned} L_0(u_0) &= -\nabla \cdot a_0 \nabla u_0 = f && \text{in } \Omega, \\ u_0 &= 0 && \text{on } \partial\Omega, \end{aligned}$$

where

$$a_0 = \frac{1}{|Y|} \int_Y a_\epsilon(I + \nabla_y \chi) dy,$$

and χ is the periodic solution of

$$\nabla_y \cdot a_\epsilon(y) \nabla_y \chi = -\nabla_y a_\epsilon(y)$$

with $\int_Y \chi_j dy = 0$. Here, $Y = \epsilon I$ and I is a unit box. The function u_1 is defined by

$$u_1(x, y) = \chi(y) \nabla u_0(x).$$

Since $u_0(x) + \epsilon u_1(x, y) \neq u_\epsilon(x)$ on $\partial\Omega$, θ^{u_ϵ} should satisfy

$$\begin{aligned} -\nabla \cdot a_\epsilon \nabla \theta^{u_\epsilon} &= 0 && \text{in } \Omega, \\ \theta^{u_\epsilon} &= -u_1 && \text{on } \partial\Omega. \end{aligned}$$

To accommodate oscillatory property of the solution u_ϵ , we need to construct an oscillatory finite element space for a good approximation of solutions. T. Hou et al. introduced the celebrated oversampling technique

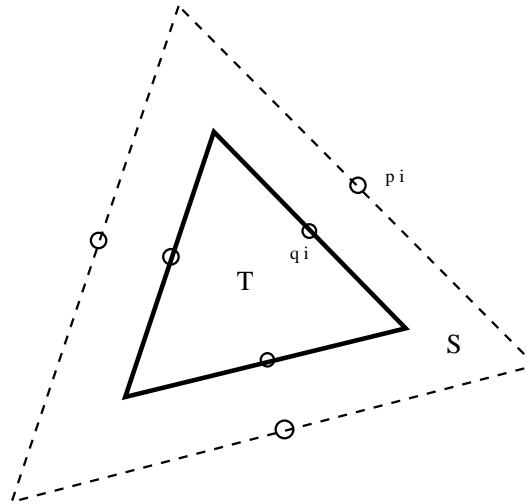


Fig. 4. A cell T and the oversampling domain S

for construction of oscillatory local basis function and developed the multiscale finite element methods(MsFEM) based on the oversampling method [5, 6, 7, 8]. Some results on the oversampling technique are briefly introduced below. Consider a local homogeneous equation on the oversampling domain S (see Fig. 4),

$$\begin{aligned} \nabla \cdot a_\epsilon \nabla \psi_\epsilon^j &= 0 \quad \text{in } S \\ \psi_\epsilon^j &= \psi^j \quad \text{on } \partial S, \end{aligned} \tag{5.3}$$

where ψ^j is the nonconforming P_1 function on S such that $\psi^j(p_i) = \delta_{ij}$. Then ψ_ϵ^j has the following representation:

$$\psi_\epsilon^j = \psi^j + \epsilon \chi \nabla \psi^j + \epsilon \eta \nabla \psi^j \quad \text{on } S, \tag{5.4}$$

where η satisfies $-\nabla \cdot (a_\epsilon \nabla \eta) = 0$ on S and $\eta = -\psi$ on ∂S . The multiscale basis ϕ_ϵ^j on T is constructed in the following way. Let $\{c_{ij}\}_{i,j=1}^3$ satisfies $\sum_{j=1}^3 c_{ij} \psi^j(q_k) = \delta_{ik}$ for the nodal point $q_k \in \partial T$. Set

$$\phi_\epsilon^i = \sum_{j=1}^3 c_{ij} \psi_\epsilon^j|_T.$$

Then the finite element space is defined as follows.

$$\begin{aligned}
S_T &= \text{span}\{\phi_\epsilon^i\}, \\
S_\epsilon^h &= \{v_\epsilon \in \oplus_{T \in \mathcal{T}_h} S_T : \text{the homogenized part } v_0 \text{ of } v_\epsilon \text{ is} \\
&\quad \text{continuous at midpoints of edges}\}.
\end{aligned}$$

6. A multiscale cell boundary element method

To introduce the CBE method, let us look at the localized problem:

$$\begin{aligned}
-\nabla \cdot a_\epsilon \nabla u_\epsilon &= f_h \quad \text{in } T, \\
[(a_\epsilon \nabla u_\epsilon) \cdot \nu] &= 0 \quad \text{on } e_p = \partial T \cap \partial T',
\end{aligned} \tag{6.1}$$

where

$$[(a_\epsilon \nabla u_\epsilon) \cdot \nu] = (a_\epsilon \nabla u_\epsilon) \cdot \nu + (a_\epsilon \nabla u_\epsilon) \cdot \nu'.$$

The solution admits a local representation as follows:

$$u_\epsilon = v_\epsilon + G \quad \text{on } T, \tag{6.2}$$

where

$$-\nabla \cdot a_\epsilon \nabla v_\epsilon = 0 \quad \text{in } T$$

with the boundary condition $v_\epsilon = u$ on ∂T , and

$$-\nabla \cdot a_\epsilon \nabla G = f_h \quad \text{in } T$$

with the boundary condition $G = 0$ on ∂T . Flux continuity yields that

$$\int_{e_p} [(a_\epsilon \nabla v_\epsilon) \cdot \nu] ds = - \int_{e_p} [(a_\epsilon \nabla G) \cdot \nu] ds, \quad p \in \mathcal{N}_h^i.$$

The multiscale CBE method is to find $v_\epsilon^h \in S_\epsilon^h$ such that

$$\int_{e_p} [(a_\epsilon \nabla v_\epsilon^h) \cdot \nu] ds = - \int_{e_p} [(a_\epsilon \nabla G) \cdot \nu] ds, \quad p \in \mathcal{N}_h^i. \tag{6.3}$$

Once v_ϵ^h is solved, we have the solution and flux formulas as follows:

$$u_\epsilon^h = v_\epsilon^h + G, \quad a_\epsilon \nabla u_\epsilon^h = a_\epsilon \nabla v_\epsilon^h + a_\epsilon \nabla G$$

on each T .

Theorem 6.1 [9] *Suppose $0 < \epsilon \ll h$. Let u_ϵ is the exact solution with the homogenized solution $u_0 \in W_\infty^2(\Omega)$ and $f \in C(\Omega)$. Then we have*

$$\|u_\epsilon - u_\epsilon^h\|_{1,h} \leq C(h + \sqrt{\epsilon})(\|f\|_{\infty,\Omega} + \|u_0\|_{2,\infty,\Omega}).$$

7. Numerical results

We test convergences of the P_1 -CBE method, two different P_2^* -methods and the MsCBE. The computational domain is taken as the unit square $\bar{\Omega} := [0, 1] \times [0, 1]$ and we take an extremely non-regular triangulation (see Fig. 5), the vertices are given as

$$x_i = t_i \quad \text{and} \quad y_j = t_j^2, \quad 0 \leq i, j \leq n,$$

and a quasi-uniform triangulation,

$$x_i = t_i \quad \text{and} \quad y_j = \frac{2t_j}{1 + t_j}, \quad 0 \leq i, j \leq n,$$

where $\{t_j = j/n, j = 0, \dots, n\}$ for Examples 7.1 and 7.2. We use the uniform triangulation for multiscale problems. Triangles are then generated by bisecting each rectangle by the diagonal line. To show the mass conservation property, we consider a subdomain $D = [0, 1/2] \times [0, 1]$ and we calculate the total numerical flux on D (flux_D) by integrating the normal flux on ∂D .

Example 7.1 (The P_1 method on a geometric triangulation)

$$\begin{aligned} -\nabla \cdot (a\nabla u) &= f \quad \text{in } \Omega, \\ u &= g \quad \text{on } \partial\Omega, \end{aligned}$$

where $a(x, y) = e^{-x}$, $f(x, y) = -.11y^{-.9}$ and $u(x, y) = e^x y^{1.1}$.

Table 1 shows that numerical results coincide well with the estimate in Theorem 3.2. When a is a scalar as in this example the nonconforming P_1 finite element method with the Raviart Thomas flux recovery formula is equivalent to the P_1 nonconforming CBE. When a is a tensor, the nonconforming P_1 CBE method provides a natural flux preserving flux formulas while the P_1 NcFEM does not. For finite volume method, the flux preserving covolume generation can be very difficult for this kind of geometric mesh and it becomes severer for three dimensional domains. In Tables the rate of convergence is defined as $\alpha = \log_2(E_n/E_{n+1})$, where E_n is the L_2 or

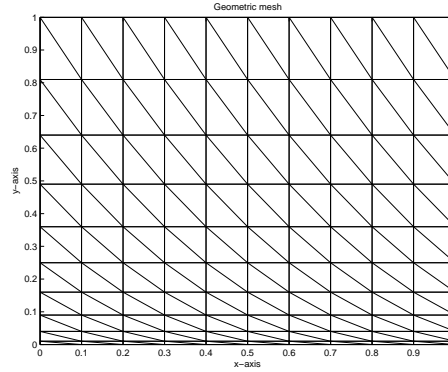


Fig. 5. A geometric mesh grading

n^2	$\ u - u_h\ _{0,h}$	α	$\ \nabla u - \nabla u_h\ _{0,h}$	α	$flux_D$
4^2	1.1362e-2		1.5041e-1		.55
8^2	3.0045e-3	1.9190	7.8822e-2	0.9322	.55
16^2	7.4702e-4	2.0079	4.0753e-1	0.9517	.55
32^2	1.8302e-4	2.0291	2.1836e-2	0.9002	.55

Table 1. Numerical results for the P_1 nonconforming method on a geometric triangulation

H^1 errors.

Example 7.2 (The P_2^* method on a quasi-uniform triangulation) We consider the following Dirichlet problem:

$$\begin{aligned} -\nabla^2 u &= f & \text{in } \Omega, \\ u &= g & \text{on } \partial\Omega, \end{aligned}$$

where $f(x, y) = 4 + 6x$ and the Dirichlet data g is given so that the exact solution is $u(x, y) = e^x \cos(y) + x^2 + x^3 + y^2$.

As shown in Tables 2 and 3, the harmonic P_2^* and modified harmonic P_2^* methods show the similar kind of convergence behaviour. As designed the modified harmonic P_2^* method preserves flux exactly. Their convergence properties are unconventional in that they show the same order of convergence in both the L_2 and H^1 -norm. The L_2 convergence is poorer than that of the FEM and it may be disappointing. However, in many practical prob-

n^2	$\ u - u_h\ _{0,h}$	α	$\ \nabla u - \nabla u_h\ _{0,h}$	α	Error in flux
4^2	3.0404 e-4		1.3019e-2		4.4105e-4
8^2	1.0316e-4	1.5594	3.3254e-3	1.9691	2.8160e-4
16^2	2.779e-5	1.8928	8.3794e-4	1.9886	1.3538e-4
32^2	7.0495e-6	1.9784	2.0986e-4	1.9974	4.3679e-5

Table 2. Numerical results for the harmonic P_2^* -method

n^2	$\ u - u_h\ _{0,h}$	α	$\ \nabla u - \nabla u_h\ _{0,h}$	α	$flux_D$
4^2	3.0295e-4		1.3014e-2		2.75
8^2	5.9258e-5	2.3540	3.3055e-3	1.9771	2.75
16^2	1.2040e-5	2.2991	8.3086e-4	1.9922	2.75
32^2	2.7165e-6	2.1481	2.0812e-4	1.9972	2.75

Table 3. Numerical results for the modified harmonic P_2^* -method

lems we are more interested in the flux ∇u than the potential u , so that this kind of convergence property will be still useful. As shown in Example 7.4 flux conservation property can be more important when we solve time dependent problems. Moreover, the modified P_2^* CBE is a unique substantial flux preserving second order method, at least to author's best knowledge. According to our experiments, two methods yield very little difference in solutions for problems as in Example 7.4 since the error in flux between the P_2^* method and modified P_2^* method is small enough.

Example 7.3 (A multiscale elliptic problem) We consider the following (quasi-one-dimensional) model problem [1]:

$$\begin{aligned}
 -\nabla \cdot \left(a_\epsilon \left(\frac{x}{\epsilon} \right) \nabla u_\epsilon \right) &= f \quad \text{in } \Omega = (0, 1)^2, \\
 u_\epsilon|_{\Gamma_D} &= 0 \quad \text{on } \Gamma_D := \{x_1 = 0\} \cup \{x_1 = 1\}, \\
 n \cdot \left(a_\epsilon \left(\frac{x}{\epsilon} \right) \nabla u_\epsilon \right)|_{\Gamma_N} &= 0 \quad \text{on } \Gamma_N := \partial\Omega \setminus \Gamma_D,
 \end{aligned}$$

where

$$a(y) = \frac{1}{2 + \cos 2\pi y_1}, \quad y = (y_1, y_2) \in Y = (0, 1)^2,$$

and $f(x) = 1$. The exact solution is given analytically as follows:

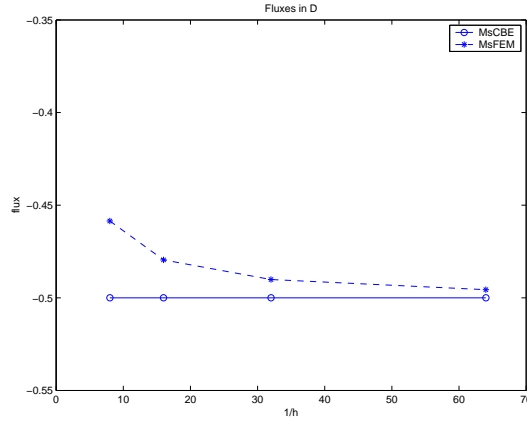


Fig. 6. Plots of flux_D^h for the MsCBE(solid line) and MsFEM(dotted line)

$$u_\epsilon(x_1, x_2) = -x_1^2 - \frac{\epsilon}{2\pi} x_1 \sin\left(\frac{2\pi x_1}{\epsilon}\right) - \frac{\epsilon^2}{4\pi^2} \left(\cos\left(\frac{2\pi x_1}{\epsilon}\right) - 1\right) + 2x_1 + \frac{\epsilon}{2\pi} \sin\left(\frac{2\pi x_1}{\epsilon}\right).$$

In implementing MsCBE, there are two processes.

- Construction of the local basis and bubble function in (5.3) and (6.2) (the fine scale solver), which is parallelizable.
- The coarse scale CBE solver (6.3).

N	$\ u_\epsilon - u_\epsilon^h\ _{0,h}$	α	$\ \nabla(u_\epsilon - u_\epsilon^h)\ _{1,h}$	α	flux_D^h
8	2.25 e-3		9.28 e-3		-5.00 e-1
16	5.99 e-4	1.91	3.73 e-3	1.15	-5.00 e-1
32	1.49 e-4	2.01	1.65 e-3	1.18	-5.00 e-1
64	2.40 e-5	2.63	6.89 e-4	1.26	-5.00 e-1

Table 4. Convergence of the MsCBE; local solver: P_1 -CBE, $\epsilon = 1/64$, $\text{dist}(K, \partial S) = 1/32$, $h_G = h_\phi = h/32$.

In Table 4 we use the fine scales of $h_\phi = h_G = h/32$ for construction of basis and the Green bubble function. For the fine scale solver of local basis, the nonconforming P_1 CBE method is used on a oversampling domain $S \supset T$ such that $\text{dist}(T, \partial S) \geq 2\epsilon$. As shown in Table 4, the rate of convergence coincides with the estimate in Theorem 6.1. We also observe that our method is free from the ϵ - h resonance as in [8] and the multiscale finite

	$t = .2$	$t = .4$	$t = .6$	$t = .8$	$t = 1$	$flux_D^h$
$\ S - S_h^{MsCBE}\ _\infty$	1.2477 e-3	1.1678 e-3	1.2108 e-3	1.2965 e-3	1.5048 e-3	-.50000
$\ S - S_h^{MsFEM}\ _\infty$	1.4471 e-1	3.2593 e-1	5.4479 e-1	7.9053 e-1	1.0404 e 0	-.48588

Table 5. Error in S as time evolves

element method yields almost the same numbers as the MsCBE except the flux. Fig. 6 shows the convergence of flux at each level of discretization for the MsCBE and MsFEM [7, 6].

Example 7.4 (A convection diffusion equation) We consider a coupled problem of a multiscale elliptic equation and a convection diffusion equation:

$$\begin{aligned}
 -\nabla \cdot (a_\epsilon(\mathbf{x})\nabla u_\epsilon) &= 1 \quad \text{in } \Omega = (0, 1)^2, \\
 u_\epsilon|_{\Gamma_D} &= 0 \quad \text{on } \Gamma_D := \{x = 0\} \cup \{x = 1\}, \\
 n \cdot (a_\epsilon(\mathbf{x})\nabla u_\epsilon)|_{\Gamma_N} &= 0 \quad \text{on } \Gamma_N := \partial\Omega \setminus \Gamma_D, \\
 \frac{\partial S}{\partial t} &= -\sigma \cdot \nabla S + 0.01\Delta S \quad \text{in } \Omega.
 \end{aligned}$$

where $\sigma = -a_\epsilon \nabla u_\epsilon$. Here, we take $\epsilon = 1/20$ and the exact solution u_ϵ is the same as in Example 7.3.

We consider the MsCBE and MsFEM with a 20×20 uniform triangulation (coarse triangulation) to produce the convective vector field $\sigma_h = a_\epsilon \nabla u_{h,\epsilon}$. To maintain flux conservation property, we use the CBE method for generation of local basis and the bubble function with fine mesh of size, $1/400$ (This corresponds to a 20×20 triangulation for a triangle T). After solving σ_h , we apply those σ_h to solve the convection diffusion equation:

$$\frac{\partial S_h}{\partial t} = -\sigma_h \cdot \nabla S_h + 0.01\Delta S_h \quad \text{in } \Omega.$$

For the convection diffusion equation, we use the FV method with a 40×40 uniform rectangular mesh and the 4th order RK with a time step, $\Delta t = 1/100$.

In Table 5, the exact solution S means that it is obtained by solving the convection diffusion equation with the the exact σ . Numerical results in Table 5 clearly show that flux conserving vector fields produce much more accurate approximate density S_h .

Acknowledgment The authors would like to express sincere thanks to a referee whose invaluable and detailed comments led to the improved version

of the paper.

References

- [1] Abdulle A. and E. W., *Finite difference HMM for homogenization problems*. J. Comput. Phys. **191** (2003), 18–39.
- [2] Bensoussan A., Lions J.-L. and Papanicolaou G., *Asymptotic Analysis for Periodic Structures*. North. Holland, Amsterdam, 1978.
- [3] Brenner S.C. and Scott L.R., *The Mathematical Theory of Finite Element Methods*. Springer-Verlag, New York, 1994.
- [4] Brezzi F., Lipnikov K. and Simoncini V., *A family of mimetic finite difference methods on polygonal and polyhedral meshes*. Math. Model Methods Appl. Sci. **15** (2005), 1533–1551.
- [5] Chen Z. and Hou T.Y., *A mixed multiscale finite element method for elliptic problems with oscillating coefficients*. Math. Comp. **72** (2003), 541–576.
- [6] Efendiev Y., Hou T.Y. and Wu X., *Convergence of a nonconforming multiscale finite element method*. SIAM J. Numer. Anal. **37** (2000), 888–910.
- [7] Hou T.Y. and Wu X.H., *A multiscale finite element method for elliptic problems in composite materials and porous media*. J. Comput. Phys. **134** (1997), 169–189.
- [8] Hou T.-Y., Wu X.-H. and Zhang Y., *Removing the cell resonance error in the multiscale finite element method via a Petrov-Galerkin formulation*. Commun. Math. Sci. **2** (2004), 185–205.
- [9] Jeon Y., *A multiscale cell boundary element method for elliptic PDEs*. submitted.
- [10] Jeon Y. and Park E.-J., *A cell boundary element method for convection-diffusion equations*. Communications on Pure and Applied Analysis (2) **5** (2006), 309–319.
- [11] Jeon Y. and Park E.-J., *Nonconforming cell boundary element methods for elliptic problems on triangular mesh*. to appear in Appl. Numer. Math.
- [12] Jeon Y., Park E.-J. and Sheen D., *A cell boundary element method for elliptic problems*. Numerical Methods for Partial Differential Equations (3) **21** (2005), 496–511.
- [13] Jeon Y. and Sheen D., *Analysis of a cell boundary element method*. Advances in Computational Mathematics (3) **22** (2005), 201–222.
- [14] Jikov V.V., Kozlov S.M. and Oleinik O.A., *Homogenization of Differential Operators and Integral Functionals*. Springer-Verlag, Berlin, Heidelberg, 1994.
- [15] Knabner P. and Angermann L., *Numerical Methods for Elliptic and Parabolic Partial Differential Equations*. Springer, 2003.

Y. Jeon
Department of Mathematics
Ajou University
Suwon 443-749, Korea
E-mail: yjeon@ajou.ac.kr

E. Park
Department of Mathematics
Yonsei University
Seoul, Korea
E-mail: ejpark@yonsei.ac.kr